Supplementary information

Two Ni/Ce complexes based on bicompartmental ligands with field supported slow magnetic relaxation

Lenka Krešáková[a], Miroslava Litecká[b], Itziar Oyarzabal[c,d], Ján Titiš[e], Michaela Červeňáková[e] Elizabeth Hillard[f], Jerome Robert[g], Juraj Černák*[a]

[a]*Department of Inorganic Chemistry, Faculty of Science, P. J. Šafárik University in Košice, Moyzesova 11, 041 54 Košice, Slovakia*

[b]*Department of Materials Chemistry, Institute of Inorganic Chemistry of the Czech Academy of Sciences, Husinec-Řež, 25068 Řež, Czech Republic*

[c]*BCMaterials - Basque Center for Materials, Applications and Nanostructures, UPV/EHU Science Park, 48940 Leioa, Spain*

[d]*IKERBASQUE, Basque Foundation for Science, 48009 Bilbao, Spain*

[e]*Department of Chemistry, Faculty of Natural Sciences, University of SS Cyril and Methodius*

Nám. J. Herdu 2, 91701 Trnava, Slovakia

[f]*Univ. Bordeaux, CNRS, Bordeaux INP, ICMCB, UMR 5026, F-33600 Pessac, France*

[g]*Université de Strasbourg, CNRS, Institut de Physique et Chimie des Matériaux de Strasbourg (IPCMS), UMR 7504, F-67000 Strasbourg, France*

**Correspondence e-mail: juraj.cernak@upjs.sk*

Analytical data

H_2(*o-van-dap*)

Anal. [%], calculated for $C_{19}H_{22}N_2O_4$: C, 66.65; H, 6.48; N, 8.18; found: C, 67.01; H, 6.48; N, 8.23.

FT-IR (cm^{-1}): 3054w, 2993w, 2962w, 2937w, 2900w, 2834w, 2595br, 1623s, 1471m, 1461s, 1422m, 1345w, 1329w, 1252s, 1170m, 1139m, 1078s, 1039m, 998w, 967m, 937w, 913w, 873w, 838s, 776s, 731s, 636m, 615w, 590w, 572w, 604w, 440m, 416w.

^{1}H NMR (ppm): 1.32d (3H); 3.74s (5H); 3.76s (3H); 3.78m (1H); 6.79q (2H); 6.98dd (1H); 7.00m (1H); 7.03d (2H); 8.54s (1H); 8.56s (1H); 13.57s (OH); 13.59s (OH).

^{13}C NMR (ppm): 19.9 ($CHCH_3$); 55.5 (OCH_3); 55.7 (OCH_3); 63.4 ($CHCH_3$); 64.1 (CHCN); 114.8 (ArC3); 117.8 (ArC4); 117.9 (ArC5); 118.2 (ArC6); 118.3 (ArC5); 123.1 (ArC6); 123.2 (ArC4); 147.9 (ArC1-OCH_3); 148.0 (ArC18-OCH_3). 151.2 (ArC7-OH); 151.5 (ArC16OH); 165.3 (C=N); 167.1 (C=N).

H_2(*o-van-dmdap*)

Anal. [%], calculated for $C_{21}H_{26}N_2O_4$: C, 68.09; H, 7.07; N, 7.56; found: C, 68.44; H, 7.18; N, 7.46.

FT-IR (cm^{-1}): 3077w, 3005w, 2956w, 2890w, 2588br, 1626s, 1469s, 1458s, 1440m, 1418m, 1393w, 1372w, 1338m, 1286w, 1268w, 1247s, 1167m, 1154w, 1077m, 1037s, 974m, 966w, 920w, 870m, 840m, 835w, 782s, 740s, 727s, 636m, 580w, 565w, 548w, 535w, 503, 438w, 416w.

^{1}H NMR (ppm): 0.99s (3H); 3.49d (1H); 3.78d (3H); 6.81td (1H); 7.02m (1H); 7.05m (1H); 8.53s (2H); 13.88s (OH).

^{13}C NMR (ppm): 23.6 (CCH_3); 35.8 (CCH_3); 55.7 (OCH_3); 66.6 (NCH_2); 114.7 (ArC3); 117.8 (ArC4); 118.3 (ArC6); 123.2 (ArC5); 148.0 (ArC1-OCH_3); 151.7 (ArC7-OH); 166.8 (C=N).

[Ni(*o-van-dap*)Ce(H_2O)(NO_3)$_3$](1)

Anal [%], calculated for $C_{19}H_{22}N_5O_{14}NiCe$: C, 30.71; H, 2.98; N, 9.42; found: C, 31.02; H, 3.19; N, 9.27.

FT-IR (cm^{-1}) (**1**): 3396br, 2988w, 2953w, 2851w, 1627m, 1608m, 1561w, 1504m, 1471s, 1459s, 1440s, 1407m, 1398m, 1334m, 1314m, 1288s, 1250s, 1233s, 1204w, 1170m, 1126w, 1099w, 1078m, 1049w, 1032m, 968m, 945w, 883w, 856m, 816m, 786m, 737s, 684w, 665w, 637w, 626w, 585w, 546w, 530w, 489w, 472w, 441w, 416w.

[Ni(H_2O)$_2$(*o-van-dmdap*)Ce(NO_3)$_3$] (2)

Anal [%], calculated for $C_{21}H_{28}N_5O_{15}NiCe$: C, 31.96; H, 3.58; N, 8.87; found: C, 31.73; H, 3.29; N, 8.80.

FT-IR (cm^{-1}) (**2**): 3502m, 3427m, 2996w, 2949w, 1644m, 1630s, 1606m, 1561w, 1506m, 1491m, 1459s, 1453s, 1409m, 1391m, 1369w, 1325m, 1289s, 1240w, 1219s, 1168w, 1105w, 1066s, 1050w, 1024s, 1003w, 968m, 927m, 903w, 881w, 849m, 815w, 799w, 786w, 779w, 745m, 734s, 643m, 613w, 565w, 551w, 537w, 477m, 454w, 443w, 429w, 406w.

Table S1 Ni/Ce heterobimetallic complexes based on bicompartmental Schiff base type ligands derived from *o*-vanillin (or its derivatives) and various diamines, with known crystal structures.

Complex/ Refcode, Reference	**Chromophore**	**Ni···Ce distance [Å]**	**Magnetism, type of interaction**
NiCe dinuclear complexes			
[Ni(*o-van-en*)$CeCl_3(H_2O)$] BORDOE [1]	{NiO_2N_2} (D_{4h}) {CeO_5Cl_3}	3.41	field induced SMM, **NI**
[$(MeCN)_2$Ni(*o-van-pn*)$Ce(NO_3)_3(H_2O)$] [(MeCN)(H_2O)Ni(*o-van-pn*) $Ce(NO_3)_2(H_2O)_2](NO_3)\cdot 2MeCN$ IWUSOJ [2]	{NiO_2N_4} (O_h) {NiO_3N_3} {CeO_{10}}	3.61	DC, **AF,** not measured
[Ni(*o-evan-trans-dach*) $Ce(H_2O)(NO_3)_3$] MABMOT [3]	{NiO_2N_2} (D_{4h}) {CeO_{11}}	3.57	DC, **NI**
[$(MeCN)_2$Ni(*o-van-pn*)$Ce(NO_3)_3$] NOVMIW [4]	{NiO_2N_4} (O_h) {CeO_{10}}	3.56	_
[Ni(*o-van-dach*)$Ce(H_2O)(NO_3)_3$] QULYED [5]	{NiO_2N_2} (D_{4h}) {CeO_{11}}	3.35	DC, **NI**
[Ni(*o-evan-en*)$Ce(NO_3)_3$] SAQCOD [6]	{NiO_2N_2} (D_{4h}) {CeO_{10}}	3.49	DC, **NI**
Ni_2Ce trinuclear complexes			
[(Ni(*o-van-en*))$_2$ $Ce(NO_3)_2(H_2O)](NO_3)$ MEFYAA [7]	{NiO_2N_2} (D_{4h}) {CeO_{12}}	3.50	_
[(Ni(*o-hap-pn*))$_2$$Ce(NO_3)_3$] PABWEX [8]	{NiO_2N_2} (D_{4h}) {CeO_{10}}	3.44, 3.33	_
[(Ni(MeOH)(*Br-o-van-en*))$_2$ $Ce(OAc)_2]NO_3\cdot 4H_2O$ SIVLIU [9]	{NiO_4N_2} (O_h) {CeO_{10}}	3.57	DC, **AF** (J = -1.1(4) cm^{-1})
[(Ni(*o-evan-en*))$_2$$Ce(NO_3)_2](NO_3)$ XAPVER [10]	{NiO_2N_2} (D_{4h}) {CeO_{10}}	3.53, 3.57	_
Tetranuclear complexes Ni_3Ce core			
[(Ni(*o-van-dach*))$_3$$Ce(OAc)_2](OAc)$ $\cdot H_2O$ OBOGUL [11]	{NiO_2N_2} (D_{4h}) {CeO_{10}}	3.57, 3.58, 3.60	_
[(Ni(*o-van-en*))$_3$$Ce(OAc)_2](OAc)$ OBOHEW [11]	{NiO_2N_2} (D_{4h}) {CeO_{10}}	3.55, 3.56, 3.58	_

* *pn* = 1,3-diaminopropane; *o-evan* = 3-ethoxysalicylaldehyde/*o*-ethylvanillin; *trans-dach* = *trans*-1,2-diaminocyclohexane; *o-hap* = *o*-hydroxyacetophenone; *dach* = 1,2-diaminocyclohexane; *Br-o-van* = 5-bromo-*o*-vanillin; DC/AC measurements, **AF** = antiferromagnetic interaction, **F** = ferromagnetic interaction, NI = no interaction, SMM = single molecule magnet

Structural data

Table S2 Crystal data and structure refinements for **1** and **2**.

	1	**2**
Empirical formula	$C_{19}H_{22}N_5NiCeO_{14}$	$C_{21}H_{28}N_5NiCeO_{15}$
Molecular weight	743.24	789.31
Crystal system	Triclinic	Monoclinic
Space group	*P* -1	*P* 2_1
Temperature (K)	100(2)	100(2)
Cell parameters		
a (Å)	7.8894(2)	8.8746(10)
b (Å)	11.3473(2)	16.0480(2)
c (Å)	14.4942(2)	10.0771(10)
α (°)	93.723(10)	90
β (°)	92.398(2)	91.844(10)
γ (°)	101.789(2)	90
V (Å^3)	1265.50(4)	1434.43(3)
Z	2	2
D_{calc} (Mg.m^{-3})	1.951	1. 827
Abs. coeff. (mm^{-1})	15.378	13.635
Crystal colour, form	orange block	green prism
Crystal size (mm)	0.092 x 0.081 x 0.058	0.460 x 0.400 x 0.210
Radiation (Å)	CuKα (λ = 1.54184)	CuKα (λ = 1.54184)
θ range (°)	3.060 – 67.490	4.390 – 77.891
Index ranges	$-9 \le h \le 9$ $-12 \le k \le 13$ $-17 \le l \le 15$	$-9 \le h \le 11$ $-20 \le k \le 19$ $-11 \le l \le 12$
Refl. coll./ indep.	14635/4559	13419 /5473
Goodness-of-fit (F^2)	1.111	1.028
Final *R* indices	$R1 = 0.0444$	$R1 = 0.0621$
($I > 2\sigma(I)$)	w$R2 = 0.1230$	w$R2 = 0.1577$
R indices (all data)	$R1 = 0.0452$ w$R2 = 0.1237$	$R1 = 0.0622$ w$R2 = 0.1580$
Diff. peak and hole (e.Å^{-3})	$-1.674 \le \Delta\rho \le 2.502$	$-2.320 \le \Delta\rho \le 3.225$

Table S3 Results of the *SHAPE* [12] calculations defining the polyhedra shape of Ce(III) ions in complexes **1** and **2**.

Polyhedron shape	Probability for **1**	Polyhedron shape	Probability for **2**
JASPC-11	5.198	HD-10	7.063
JAPPR-11	10.759	TD-10	4.336
JCPAPR-11	**3.204**	SDD-10	4.342
JCPPR-11	8.704	**JSPC-10**	**2.951**
EBPY-11	17.375	JATDI-10	17.896
DPY-11	25.712	JMBIC-10	7.600
HP-11	36.421	JBCSAPR-10	6.265
		JBCCU-10	10.473
		PAPR-10	10.318
		PPR-10	9.211
		OBPY-10	16.777
		EPY-10	22.848
		DP-10	35.651

JASPC-11	Augmented sphenocorona J87	HD-10	Hexadecahedron (2:6:2) or (1:4:4:1)
JAPPR-11	Augmented pentagonal prism J52	TD-10	Tetradecahedron (2:6:2)
JCPAPR-11	Capped pentagonal antiprism J11	SDD-10	Staggered Dodecahedron (2:6:2)
JCPPR-11	Capped pentagonal prism J9	JSPC-10	Sphenocorona J87
EBPY-11	Enneagonal bipyramid	JATDI-10	Augmen. tridiminished icosahedron J64
DPY-11	Decagonal pyramid	JMBIC-10	Metabidiminished icosahedron J62
HP-11	Hendecagon	JBCSAPR-10	Bicapped square antiprism J17
		JBCCU-10	Bicapped cube J15
		PAPR-10	Pentagonal antiprism
		PPR-10	Pentagonal prism
		OBPY-10	Octagonal bipyramid
		EPY-10	Enneagonal pyramid
		DP-10	Decagon

Table S4 Potential hydrogen bonding interactions in **1** [Å, °].

D-H···A	***d*(D-H)**	***d*(H···A)**	***d*(D···A)**	**<(DHA)**	
O14-H14A···O13^{i}	0.84(7)	2.06(7)	2.816 (6)	149(7)	
O14-H14B···O10^{i}	0.84(6)	2.13(7)	2.959 (7)	170(8)	
C3-H3···O6^{ii}	0.95	2.59	3.407(7)	144	
C5-H5···O13^{iii}	0.95	2.50	3.369(7)	153	
C8-H8···O13^{iii}	1.01(8)	2.48(7)	3.421(7)	154(6)	
C11-H11···O8^{iv}	0.89(8)	2.59(7)	3.407(7)	154(6)	
C15-H15···O7^{v}	0.95	2.41	3.298(7)	156	
π-π	**Cg···Cg**	**α**	**β**	**γ**	**Slippage**
Cg1···Cg1^{vi}	3.676(3)	0	15.1	15.1	0.960
Cg2···Cg2^{vii}	3.629(3)	0	20.8	20.8	1.290

Symmetry codes: i: -1 + *x*, *y*, *z*; ii: 1 - *x*, - *y*, - *z*; iii: 2 - *x*, 1 - *y*, - *z*; iv: 2 - *x*, 1 - *y*, 1 - *z*; v: 1 - *x*, - *y*, 1 - *z*; vi: 1 - *x*, 1 - *y*, 1 - *z*; vii: 1 - *x*, 1 - *y*, -*z*; viii : 1 + *x*, *y*, *z*. Cg1 is the centre of gravity of the aromatic ring formed by C12-C17 atoms, Cg2 is the centre of gravity of the aromatic ring formed by C2-C7 atoms.

Table S5 Potential hydrogen bonding interactions in **2** [Å, °].

D-H···A	**d(D-H)**	**d(H···A)**	**d(D···A)**	**<(DHA)**
O14-H14B···O13^{i}	0.87	2.02	2.8194(1)	153
O15-H15A···O6^{ii}	0.84	2.02	2.8410(1)	165
O14-H14A···O9	0.87	2.01	2.7166(1)	139
O15-H15B···O12	0.84	2.06	2.7807(1)	143
C21-H21A···O9^{ii}	0.98	2.52	3.0883(1)	141
C21-H21B···O10^{iv}	0.98	2.57	3.5203(1)	163

Symmetry codes: i: *x*, *y*, -1 + *z*; ii: 1 + *x*, *y*, *z*; iii: *x*, *y*, 1 + *z*; iv: 1 - *x*, -1/2 + *y*, 1 - *z*.

Table S6. Fitting parameters for **1** and **2** from Cole-Cole plots.

Compound 1				Compound 2			
T / K	**χ_S / cm^{3}mol^{-1}**	**χ_T / cm^{3}mol^{-1}**	**α**	**T / K**	**χ_S / cm^{3}mol^{-1}**	**χ_T / cm^{3}mol^{-1}**	**α**
2	$2.61\cdot10^{-3}$	$2.17\cdot10^{-1}$	0.27	**2**	$2.06\cdot10^{-1}$	$4.76\cdot10^{-1}$	0.12
2.2	$3.03\cdot10^{-3}$	$2.01\cdot10^{-1}$	0.24	**2.1**	$2.10\cdot10^{-1}$	$4.61\cdot10^{-1}$	0.11
2.4	$3.95\cdot10^{-3}$	$1.79\cdot10^{-1}$	0.19	**2.2**	$2.17\cdot10^{-1}$	$4.46\cdot10^{-1}$	0.07
2.6	$4.33\cdot10^{-3}$	$1.63\cdot10^{-1}$	0.14	**2.3**	$2.23\cdot10^{-1}$	$4.36\cdot10^{-1}$	0.07
2.8	$5.13\cdot10^{-3}$	$1.50\cdot10^{-1}$	0.09	**2.4**	$2.21\cdot10^{-1}$	$4.24\cdot10^{-1}$	0.07
3	$5.31\cdot10^{-3}$	$1.37\cdot10^{-1}$	0.06	**2.5**	$2.24\cdot10^{-1}$	$4.14\cdot10^{-1}$	0.06
3.2	$5.38\cdot10^{-3}$	$1.30\cdot10^{-1}$	0.06	**2.6**	$2.29\cdot10^{-1}$	$4.03\cdot10^{-1}$	0.05
3.4	$5.25\cdot10^{-3}$	$1.22\cdot10^{-1}$	0.04	**2.7**	$2.23\cdot10^{-1}$	$3.95\cdot10^{-1}$	0.05
3.6	$5.89\cdot10^{-3}$	$1.16\cdot10^{-1}$	0.03	**2.8**	$2.30\cdot10^{-1}$	$3.86\cdot10^{-1}$	0.05
3.8	$4.86\cdot10^{-3}$	$1.11\cdot10^{-1}$	0.05	**2.9**	$2.29\cdot10^{-1}$	$3.78\cdot10^{-1}$	0.06
4	$7.29\cdot10^{-3}$	$1.04\cdot10^{-1}$	0.02	**3**	$2.30\cdot10^{-1}$	$3.70\cdot10^{-1}$	0.05
4.2	$5.36\cdot10^{-3}$	$9.99\cdot10^{-2}$	0.05	**3.1**	$2.32\cdot10^{-1}$	$3.63\cdot10^{-1}$	0.04
4.4	$7.05\cdot10^{-3}$	$9.52\cdot10^{-2}$	0.04	**3.2**	$2.30\cdot10^{-1}$	$3.56\cdot10^{-1}$	0.05
4.6	$4.98\cdot10^{-3}$	$9.12\cdot10^{-2}$	0.01				

Table S7 Energies of the lowest Kramer doublets (KDs) for Ce(III) ion in **1** Ce-Ni calculated using single_aniso module together with g-values, transition magnetic moments quantifying probability for the quantum tunnelling of magnetization (QTM) and deviations from the principal magnetisation axes of the first KD.

KD	ΔE (cm^{-1})	g_{xx}	g_{yy}	g_{zz}	QTM	θ(°)
1	0	0.223	1.126	3.333	0.224977068171E+00	-
2	106.97	2.547	1.896	0.507	0.615069853095E+00	12.88
3	324.71	0.035	0.637	3.247	0.381536894005E+00	12.65

Table S8 Composition of wave functions of the ground J = 5/2 state of Ce(III) ion for complex **1** Ce-Ni obtained from single_aniso calculations.

w.f.	m_J	c_i		
		Real	Imag	Weight (%)
1	**-5/2**	**-0.74183073820615E-01**	**-0.91480515575970E+00**	**84.2**
	-3/2	-0.14133661484248E-01	-0.55436599085241E-01	0.3
	-1/2	+0.53733779491727E-01	-0.13864707491421E-02	0.3
	1/2	+0.47487543187659E-01	+0.29120008604358E+00	8.7
	3/2	-0.52741391074128E-01	-0.16112330368879E+00	2.9
	5/2	+0.18886834063837E+00	+0.00000000000000E+00	3.6
2	-5/2	-0.15265538573680E-01	-0.18825039999798E+00	3.6
	-3/2	-0.16485903530430E+00	-0.39545825863510E-01	2.9
	-1/2	-0.29408558176856E+00	-0.23795534967872E-01	8.7
	1/2	+0.29611708972751E-02	+0.53670037520356E-01	0.3
	3/2	+0.56397594174211E-01	+0.96066789148342E-02	0.3
	5/2	**-0.91780804153727E+00**	**+0.00000000000000E+00**	**84.2**
3	-5/2	+0.62723504566254E-01	-0.44755280425052E-01	0.6
	-3/2	**-0.60098141078592E+00**	**-0.52740925286143E+00**	**63.9**
	-1/2	-0.33425018297691E+00	+0.27092546389582E+00	18.5
	1/2	+0.20714018235646E-01	-0.23619144843819E+00	5.6
	3/2	-0.12363228640505E+00	+0.22305120926588E+00	6.5
	5/2	+0.21988065823111E+00	+0.00000000000000E+00	4.8
4	-5/2	+0.17898796305026E+00	-0.12771379159541E+00	4.8
	-3/2	+0.23019490167215E+00	+0.10975924007131E+00	6.5
	-1/2	+0.15404931625927E+00	+0.18023395506330E+00	5.6
	1/2	+0.42944967876827E+00	+0.26396318861445E-01	18.5
	3/2	**-0.18287649770761E+00**	**+0.77839280795065E+00**	**63.9**
	5/2	-0.77053705025405E-01	+0.00000000000000E+00	0.6
5	-5/2	-0.49904738934369E-01	-0.14847094407101E-01	0.3
	-3/2	+0.61504929572269E-01	-0.39194722112717E+00	15.7
	-1/2	**+0.70627675674899E+00**	**+0.28400414426367E+00**	**57.9**
	1/2	-0.24226806547196E+00	-0.17475672486025E+00	8.9
	3/2	-0.30433019688423E+00	-0.11656045467349E+00	10.6
	5/2	-0.25487536653245E+00	+0.00000000000000E+00	6.5
6	-5/2	+0.24429319651674E+00	+0.72679344454168E-01	6.5
	-3/2	-0.32493267253814E+00	+0.24939273956552E-01	10.6
	-1/2	+0.28204233776406E+00	-0.98416706775986E-01	8.9
	1/2	**+0.75793845185729E+00**	**-0.70813228453789E-01**	**57.9**
	3/2	+0.52814956281226E-01	-0.39321248804111E+00	15.7
	5/2	-0.52066486406293E-01	+0.00000000000000E+00	0.3

Table S9 Energies of the lowest KDs for Ce(III) ion in **1** Ce calculated using single_aniso module together with g-values, transition magnetic moments quantifying probability for the quantum tunnelling of magnetization (QTM) and deviations from the principal magnetisation axes of the first KD.

KD	ΔE (cm^{-1})	g_{xx}	g_{yy}	g_{zz}	QTM	θ (°)
1	0	0.101	0.644	3.844	0.124395289130E+00	-
2	250.35	1.168	1.704	2.529	0.637899861543E+00	11.68
3	620.87	0.013	0.498	3.574	0.755956118440E+00	13.96

Table S10 Composition of wave functions of the ground J = 5/2 state of Ce(III) ion for complex **1** Ce obtained from single_aniso calculations.

w.f.	m_J	c_i		
		Real	Imag	Weight (%)
1	-5/2	+0.14640393950610E+00	-0.17361859277591E+00	5.2
	-3/2	+0.94624995867049E-01	+0.26393102247770E-01	1.0
	-1/2	+0.59934837968488E-01	+0.32989210636616E-01	0.5
	1/2	-0.81847591502576E-02	+0.38923755535843E-01	0.2
	3/2	+0.17881611475358E-01	-0.21559889958117E-01	0.1
	5/2	**+0.96525897163323E+00**	**+0.00000000000000E+00**	**93.2**
2	**-5/2**	**+0.62225206001825E+00**	**-0.73792090076975E+00**	**93.2**
	-3/2	-0.28009438792300E-01	-0.22840667368285E-03	0.1
	-1/2	-0.35032708192610E-01	-0.18835030821922E-01	0.2
	1/2	-0.13417277814031E-01	+0.67085389566463E-01	0.5
	3/2	+0.40822804845505E-01	-0.89353145510913E-01	1.0
	5/2	-0.22710686758527E+00	+0.00000000000000E+00	5.2
3	-5/2	+0.10449358504959E-01	-0.13105831405708E-01	0.0
	-3/2	**-0.83526329916726E+00**	**-0.29632029755061E+00**	**78.5**
	-1/2	-0.64077623767020E-01	+0.15365954944560E-01	0.4
	1/2	-0.16380988959093E+00	-0.35075247385192E+00	15.0
	3/2	-0.18685765206084E+00	-0.12048448480915E+00	4.9
	5/2	+0.10302050728033E+00	+0.00000000000000E+00	1.1
4	-5/2	+0.64223990130257E-01	-0.80551252636713E-01	1.1
	-3/2	+0.22282632142760E-01	-0.22121432515187E+00	4.9
	-1/2	+0.17213102593625E+00	+0.34674470076011E+00	15.0
	1/2	+0.51961184707750E-01	-0.40522705453972E-01	0.4
	3/2	**-0.28901984891574E+00**	**+0.83781741717610E+00**	**78.5**
	5/2	-0.16761619350658E-01	+0.00000000000000E+00	0.0
5	-5/2	-0.85978679764792E-02	+0.19027868110689E-01	0.0
	-3/2	+0.63415787371521E-01	-0.77299075938837E-01	1.0
	-1/2	**+0.72055046526156E+00**	**+0.49613969380034E+00**	**76.5**
	1/2	-0.26418212462044E+00	+0.66292401212274E-01	7.4
	3/2	-0.60063354141476E-01	-0.37557665862125E+00	14.5
	5/2	-0.73262735959274E-01	+0.00000000000000E+00	0.5
6	-5/2	+0.30167484721100E-01	-0.66763398634601E-01	0.5
	-3/2	+0.31752586834825E+00	+0.20938661885781E+00	14.5
	-1/2	+0.16919401047211E+00	-0.21344850475757E+00	7.4
	1/2	**-0.15542385969867E+00**	**-0.86092449862328E+00**	**76.5**
	3/2	-0.96554458213686E-01	+0.25960467846139E-01	1.0
	5/2	-0.20880208173413E-01	+0.00000000000000E+00	0.0

Table S11 Energies of the lowest KDs for Ce(III) ion in **2** Ce-Zn calculated using single_aniso module together with g-values, transition magnetic moments quantifying probability for the quantum tunnelling of magnetization (QTM) and deviations from the principal magnetisation axes of the first KD.

KD	ΔE (cm^{-1})	g_x	g_y	g_z	QTM	θ(°)
1	0	0.382	0.855	3.648	0.206389976697E+00	-
2	357.80	1.026	1.712	2.580	0.643679151676E+00	5.92
3	486.70	0.324	0.701	3.502	0.446138807446E+00	5.33

Table S12 Composition of wave functions of the ground $J = 5/2$ state of Ce(III) ion for complex **2** Ce-Zn obtained from single_aniso calculations.

w.f.	m_J	c_i		
		Real	Imag	Weight (%)
1	**-5/2**	**+0.22046303572929E+00**	**+0.68253315775951E+00**	**51.4**
	-3/2	+0.56134729276744E-03	-0.10238399207934E+00	1.0
	-1/2	+0.25406542049287E-01	-0.15369447414623E+00	2.4
	1/2	+0.62634584079162E-01	-0.14371310786496E+00	2.5
	3/2	-0.13732227414324E+00	+0.17507982766282E-01	1.9
	5/2	**+0.63800765888632E+00**	**+0.00000000000000E+00**	**40.7**
2	**-5/2**	**+0.19610460111640E+00**	**+0.60712169945026E+00**	**40.7**
	-3/2	+0.25548365506701E-01	+0.13605593472468E+00	1.9
	-1/2	-0.11750394437307E+00	+0.10377558222406E+00	2.5
	1/2	+0.13844490572140E+00	-0.71417727529022E-01	2.4
	3/2	-0.97255040881322E-01	+0.32003969631008E-01	1.0
	5/2	**-0.71725550673381E+00**	**+0.00000000000000E+00**	**51.4**
3	-5/2	-0.56495394753739E-01	-0.12596174782859E+00	1.9
	-3/2	**-0.33478800618921E+00**	**+0.45563312668531E+00**	**32.0**
	-1/2	+0.20465511169838E+00	+0.31545484440328E-01	4.3
	1/2	**-0.11828542989138E+00**	**-0.52446588937647E+00**	**28.9**
	3/2	**-0.52544789797018E+00**	**-0.23029482199939E+00**	**32.9**
	5/2	+0.13835112450418E-01	+0.00000000000000E+00	0.0
4	-5/2	-0.56618187435197E-02	-0.12623555576183E-01	0.0
	-3/2	**-0.42515957334788E+00**	**-0.38518895824763E+00**	**32.9**
	-1/2	**+0.52694437244812E+00**	**-0.10670305775315E+00**	**28.9**
	1/2	+0.11253515662782E+00	+0.17382367790692E+00	4.3
	3/2	**-0.27872562772093E+00**	**+0.49193147839098E+00**	**32.0**
	5/2	-0.13805104722734E+00	+0.00000000000000E+00	1.9
5	-5/2	-0.19405609716046E+00	+0.87201880667067E-01	4.5
	-3/2	-0.93701672688782E-01	-0.45826761118387E+00	21.9
	-1/2	-0.84035507524611E-01	+0.33557963764055E-01	0.8
	1/2	**-0.48443845347757E+00**	**-0.61347575695997E+00**	**61.1**
	3/2	+0.29713229540975E+00	+0.12025267269595E+00	10.3
	5/2	-0.11823420372248E+00	+0.00000000000000E+00	1.4
6	-5/2	+0.10784595508330E+00	-0.48462120850540E-01	1.4
	-3/2	+0.22173631777259E+00	-0.23147637799704E+00	10.3
	-1/2	**+0.19042197484227E+00**	**-0.75813757943241E+00**	**61.1**
	1/2	-0.90406831208341E-01	+0.38351717762215E-02	0.8
	3/2	-0.10236693750976E+00	-0.45641014104875E+00	21.9
	5/2	-0.21274852844486E+00	+0.00000000000000E+00	4.5

Table S13 CAS(8,5)-NEVPT2 transition energies for complex **2** La-Ni.

Root	Mult	ΔE (cm^{-1})
0	3	0
1	3	9228.2
2	3	9633.7
3	3	13891.8
0	1	14590.6
1	1	16593.1

4	3	17113.7
5	3	19414.1
6	3	19532.4
2	1	24945.9
3	1	25399.4
7	3	29360.2
4	1	29508.8
6	1	30096.8
5	1	30588.8
8	3	31435.1
9	3	32093.8
7	1	35093.0
8	1	35422.9
9	1	40915.0
10	1	41109.2
11	1	41805.2
12	1	42156.5
13	1	42562.0
14	1	67532.4

Table S14 Calculated (CAS(8,5)-NEVPT2) contributions to the SH parameters in **2** La-Ni.

Root	Mult	D (cm^{-1})	E (cm^{-1})
1	3	22.335	22.577
2	3	21.408	-21.400
3	3	-30.140	0.174
4	3	0.007	0.002
5	3	0.190	-0.190
6	3	0.219	0.227
7	3	0.004	-0.004
8	3	0.022	-0.021
9	3	0.026	0.027
0	1	-0.015	-0.012
1	1	-0.001	0.001
2	1	-7.318	-7.359
3	1	-7.179	7.176
4	1	11.910	-0.020
5	1	-0.001	-0.001
6	1	-0.002	-0.002
7	1	-0.120	0.049
8	1	-0.091	-0.029
9	1	-0.107	0.122
10	1	-0.017	0.074
11	1	-0.423	0.419
12	1	-0.009	-0.412
13	1	1.030	-0.187
14	1	-0.000	-0.000

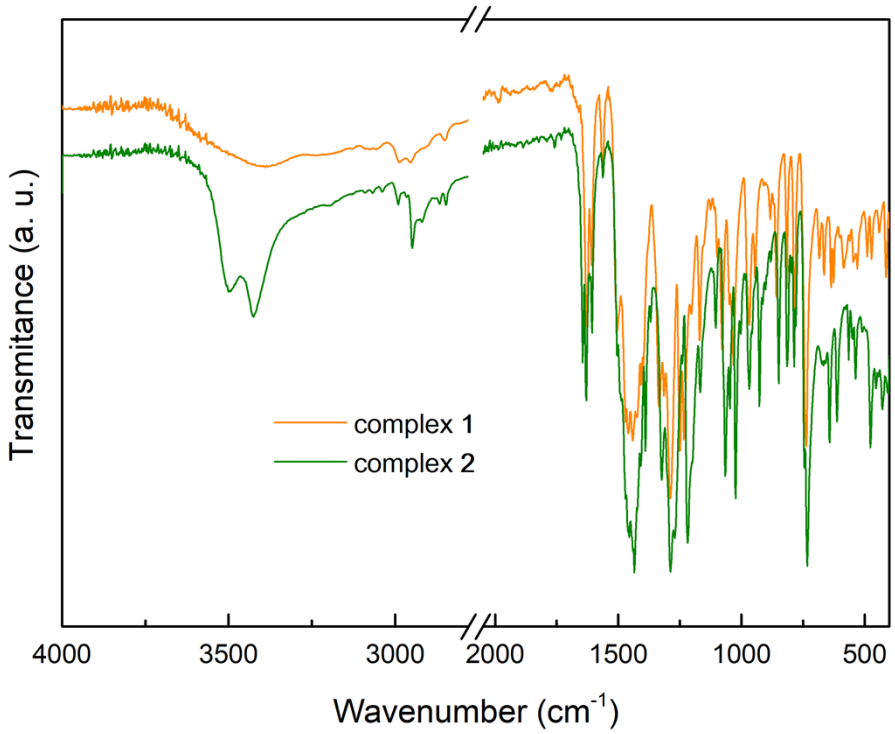

Figure S1 Comparison of the IR spectra of two Ni(II)/Ce(III) complexes: [Ni(*o-van-dap*)Ce(H_2O)(NO_3)$_3$] (**1**) and [Ni(H_2O)$_2$(*o-van-dmdap*)Ce(NO_3)$_3$] (**2**).

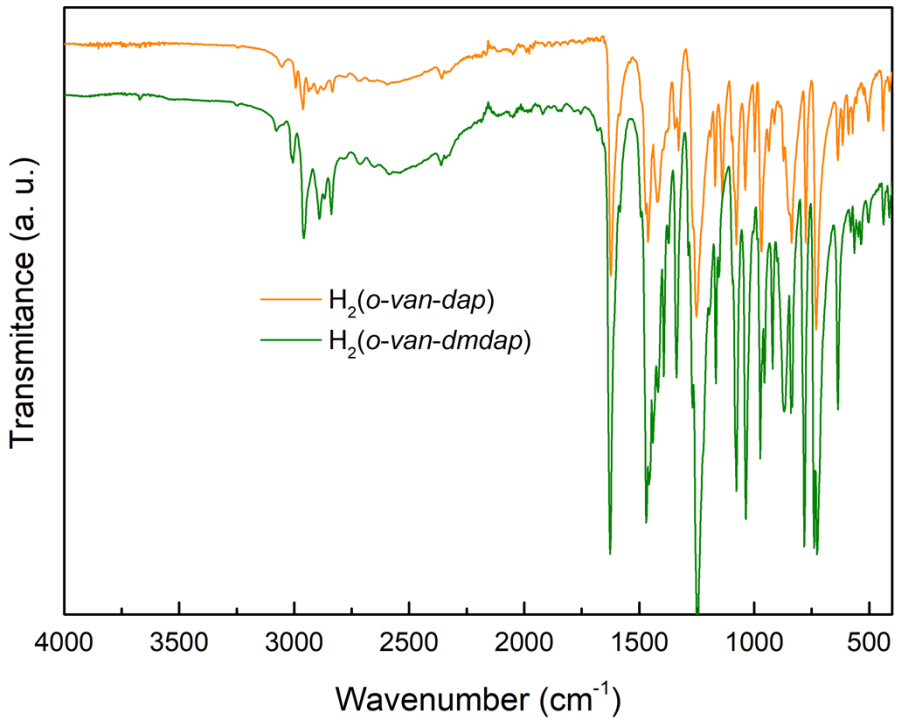

Figure S2 Comparison of the IR spectra of the Schiff base ligands.

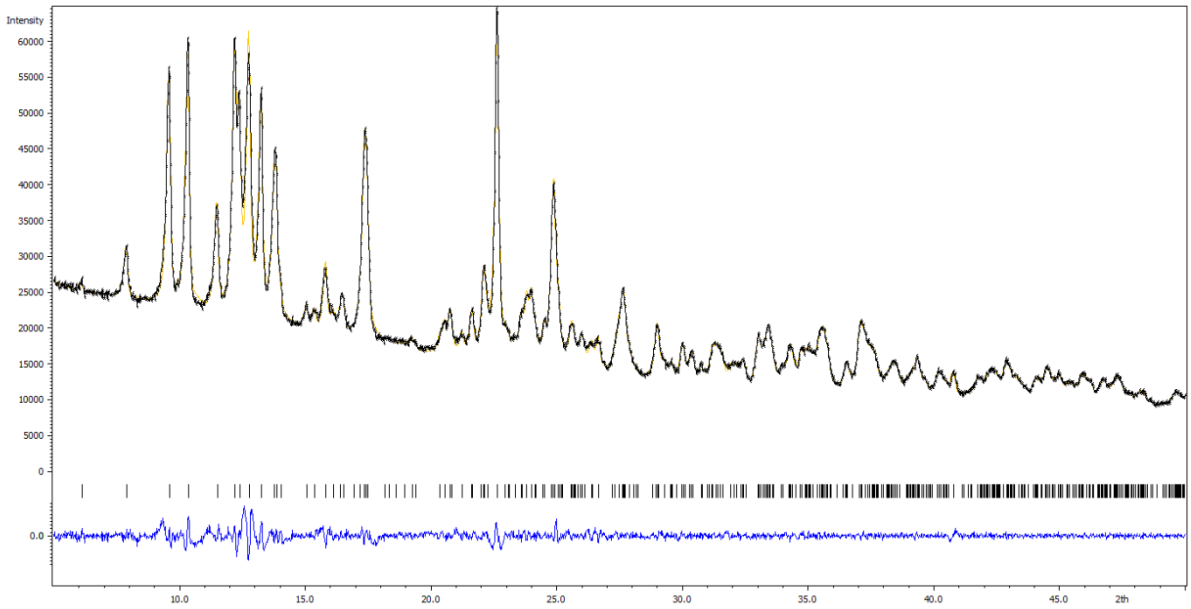

Figure S3 LeBail refinement of the measured powder diffraction pattern of complex **1**. Yellow line represents the refined pattern, black line represents the measured powder diffraction pattern, while the blue line shows the difference between the observed and calculated intensities. The refined cell lengths for triclinic *P*-1 space group are a = 7.9163(11), b = 11.5406(11), c = 14.5707(13) Å and V = 1292.1(2) Å^3, the values from appropriate low-temperature (100 K) CIF file are: a = 7.8894(2), b = 11.3473(2), c = 14.4942(2) Å and V = 1265.50(4) Å^3. We note that the experimental powder diffraction data were collected at room temperature. The resulting R values are $R(p)$ = 0.0176, $R(wp)$ = 0.0235 and goodness of fit is 3.31.

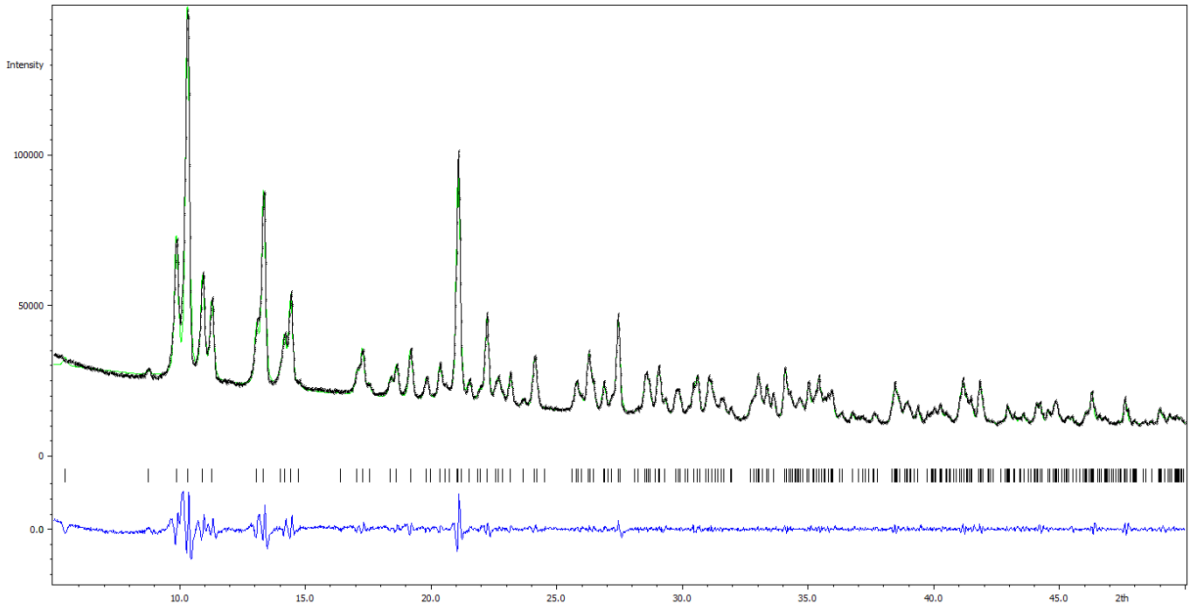

Figure S4 LeBail refinement of the measured powder diffraction pattern of complex **2**. Green line represents the refined pattern, black line represents the measured powder diffraction pattern, while the blue line shows the difference between the observed and calculated intensities. The refined cell lengths for monoclinic $P2_1$ space group are a = 8.9526 (12), b = 16.1888(10), c = 10.1005 (11) Å and V = 1463.6(2) Å^3, the values from appropriate low-temperature (100 K) CIF file are: a = 8.8746(10), b =

16.048(2), c = 10.0771(10) Å and V = 1434.43(3) Å^3. We note that the experimental powder diffraction data were collected at room temperature. The resulting R values are $R(p)$ = 0.0656, $R(wp)$ = 0.0308 and goodness of fit is 4.41.

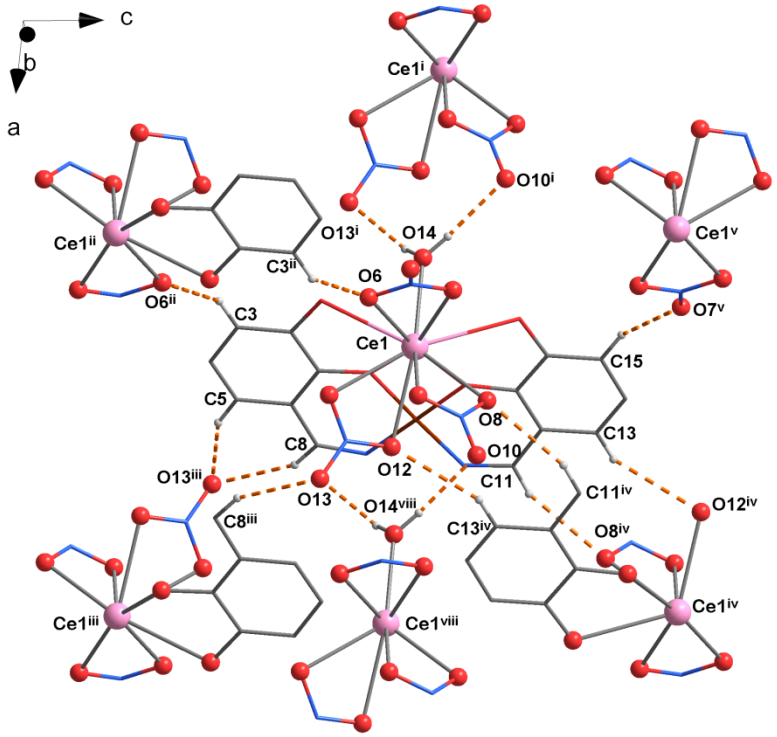

Figure S5 View on the O-H···O and weak C-H···O type hydrogen bonds (orange dashed lines) in **1**. Only atoms relevant for hydrogen bonding interactions are shown. Symmetry codes: i: -1 + x, y, z; ii: 1 - x, - y, - z; iii: 2 - x, 1 - y, - z; iv: 2 - x, 1 - y, 1 - z; v: 1 - x, - y, 1 - z; vi: 1 - x, 1 - y, 1 - z; vii: 1 - x, 1 - y, -z; viii : 1 + x, y, z.

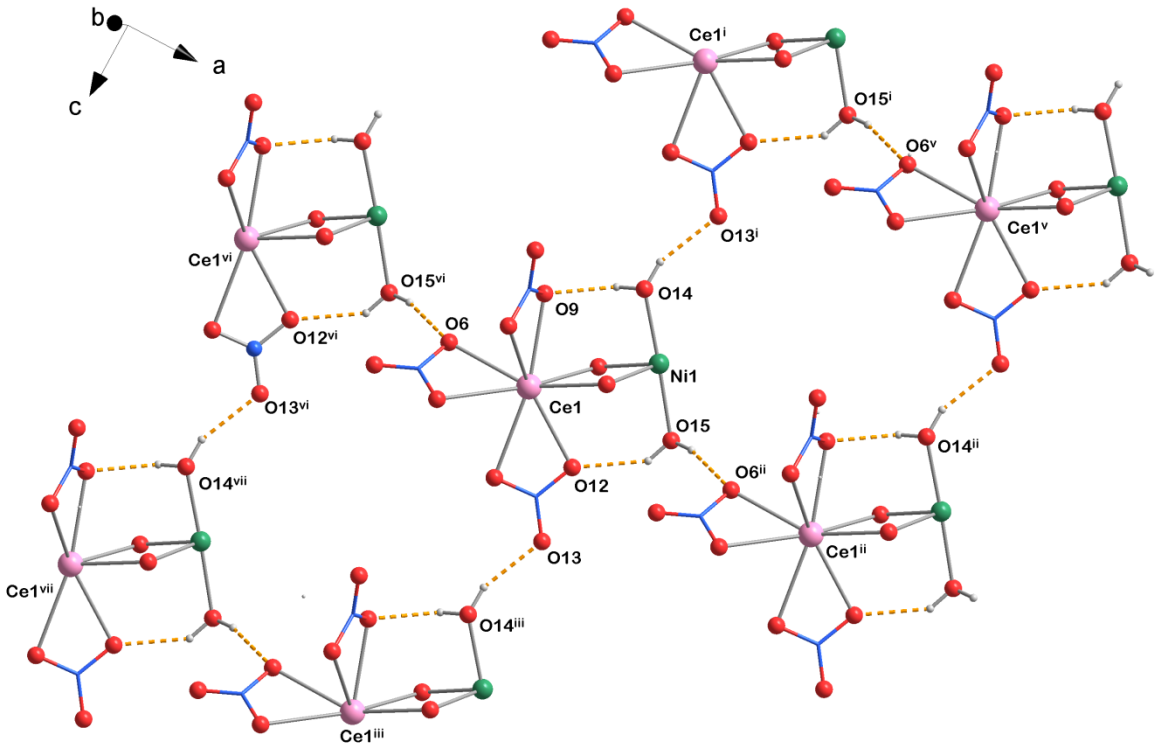

Figure S6 View on the O-H···O type intramolecular and intermolecular hydrogen bonds (orange dashed lines) in **1**. Only atoms relevant for hydrogen bonding interactions are shown. Symmetry codes: i: *x*, *y*, -1 + *z*; ii: 1 + *x*, *y*, *z*; iii: *x*, *y*, 1 + *z*; iv: 1 - *x*, -1/2 + *y*, 1 - *z*; v: 1 + *x*, *y*, -1 + *z*; vi: -1 + *x*, *y*, *z*; vii: -1 + *x*, *y*, 1 + *z*.

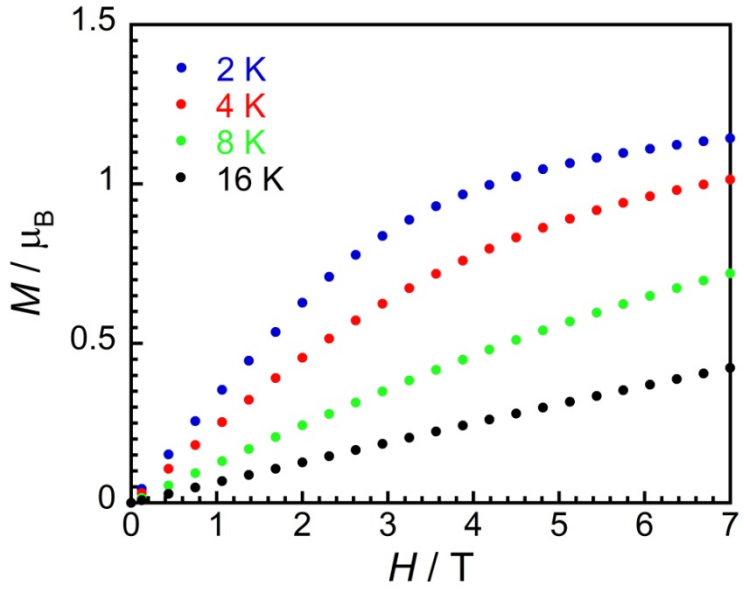

Figure S7 Field dependent magnetization curves at different temperatures for **1**.

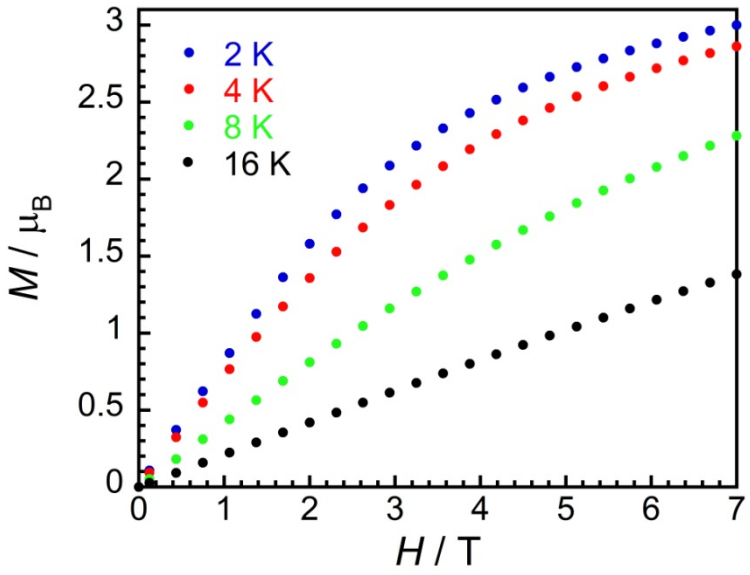

Figure S8 Field dependent magnetization curves at different temperatures for **2**.

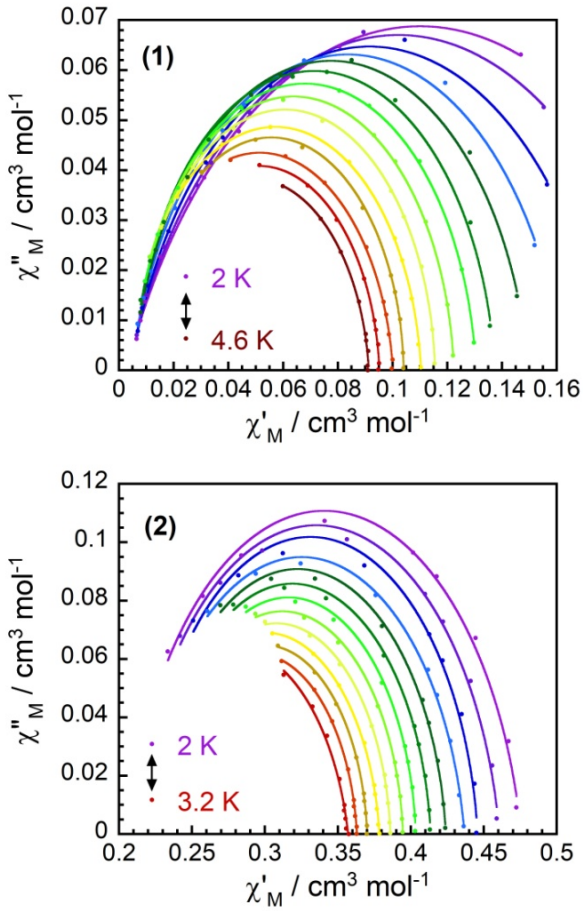

Figure S9 Cole-Cole plots for **1** and **2**. The experimental data are denoted by circles; solid lines represent the best fit to the Debye model.

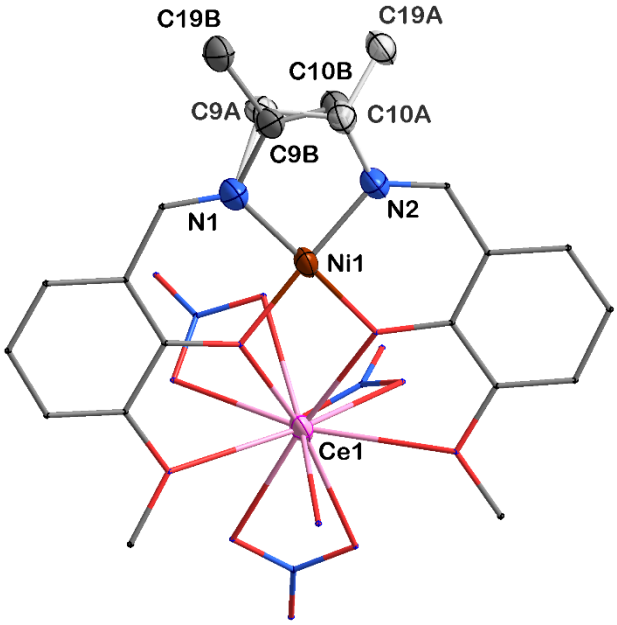

Figure S10 View on the disordered 1,2-diaminopropane fragment in the complex **1** (C9A/C9B, C10A/C10B a C19A/C19B) with occupation factors in 0.38 : 0.62 *ratio*. The thermal ellipsoids for disordered C atoms and appropriate N atoms of the fragment, Ni and Ce central atoms were drawn with 50 % probability level. The rest of the molecule is depicted in wire and stick model. Hydrogen atoms are omitted for clarity.

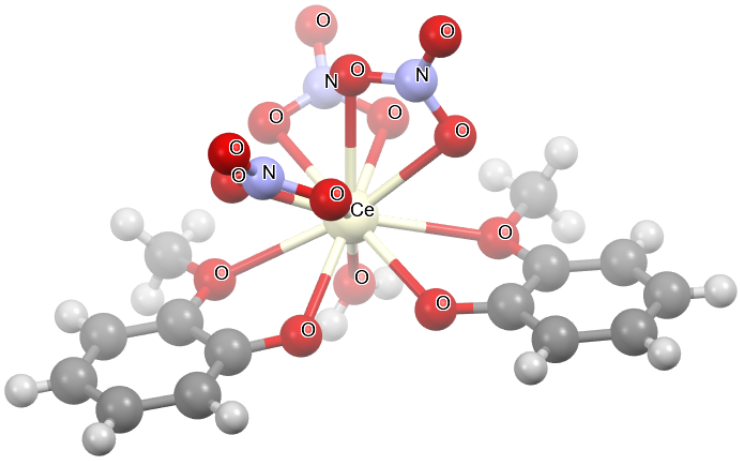

Figure S11 Truncated molecular structure of the complex **1** (**1** Ce = $[CeL_2(NO_3)_3H_2O]^{2-}$).

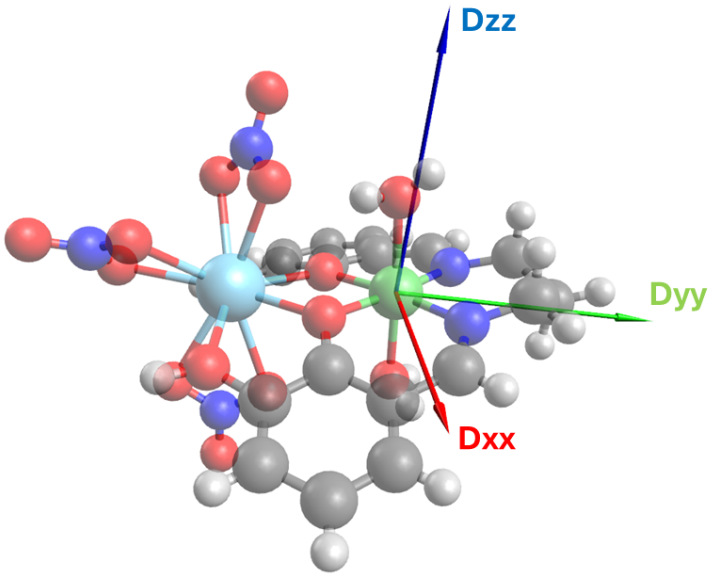

Figure S12 Orientation of the principal axes of the *D*-tensor in structure **2** La-Ni.

References

[1] A. Vráblová, M. Tomás, L. R. Falvello, Ľ. Dlháň, J. Titiš, J. Černák, R. Boča, *Dalton Trans*., 2019, **48**, 13943. https://doi.org/10.1039/c9dt02122a.

[2] T. D. Pasatoiu, J.-P. Sutter, A. M. Madalan, F. Z. Ch. Fellah, C. Duhayon, M. Andruh, *Inorg. Chem*., 2011, **50**, 5890. https://doi.org/10.1021/ic2004276.

[3] A. Jana, S. Majumder, L. Carrella, M. Nayak, T. Weyhermueller, S. Dutta, D. Schollmeyer, E. Rentschler, R. Koner, S. Mohanta, *Inorg. Chem*., 2010, **49**, 9012. https://doi.org/10.1021/ic101445n.

[4] J. S. Elias, M. Risch, L. Giordano, A. N. Mansour, Y. Shao-Horn, *J. Am. Chem. Soc.*, 2014, **136**, 17193. https://doi.org/10.1021/ja509214d.

[5] H.-R. Wen, S.-J. Liu, X.-R. Xie, J. Bao, C.-M. Liu, J.-L. Chen, *Inorg. Chim. Acta,* 2015, **435**, 274. http://dx.doi.org/10.1016/j.ica.2015.07.009.

[6] R. Koner, H.-H. Lin, H.-H. Wei, S. Mohanta, *Inorg. Chem*., 2005, **44**, 3524. https://doi.org/10.1021/ic048196h.

[7] S. A. Güngör, M. Kose, *J. Mol. Struct*., 2017, **1150**, 274. https://doi.org/10.1016/j.molstruc.2017.08.091.

[8] S. Ghosh, A. Ghosh, *Inorg. Chim. Acta*, 2016, **442**, 64. https://doi.org/10.1016/j.ica.2015.11.029.

[9] B. Cristóvao, J. Klak, R. Pelka, B. Miroslaw, Z. Hnatejko, *Polyhedron*, 2014, **68**, 180. http://dx.doi.org/10.1016/j.poly.2013.10.019.

[10] Y. Sui, R.-H. Hu, D.-S. Liu, Q. Wu, *Inorg. Chem. Commun*., 2011, **14**, 396. https://doi.org/10.1016/j.inoche.2010.12.010.

[11] H. Nagae, K. Sakamoto, S. Fujiwara, T. Schindler, Y. Kon, K. Sato, J. Okuda, K. Mashima, *Chem. Commun*., 2021, **57**, 11169. https://doi.org/10.1039/D1CC04540G.

[12] M. Llunell, D. Casanova, J. Cirera, P. Alemany, S. Alvarez, SHAPE Program, version 2.1, Universitat de Barcelona (2013).